Iranian Society of Acoustics and Vibration
The 10th ISAV2020 International Conference on Acoustics and Vibration
17-18 Feb 2021 Tehran - Iran
University of Tehran

Evaluation of Quasi-Two-Dimensional Integral Surface Sound Simulation Method

Alireza Maleki, Majid Mesbah[a*], Arman Mohseni[a]

[a] *Assistant Professor, Mechanical and Energy Engineering Department, Shahid Beheshti University, A. C., Tehran, Iran*

** Corresponding author e-mail: m_mesbah@sbu.ac.ir*

Abstract

In this research a quasi-two-dimensional integral surface method able to simulate the acoustic domains is evaluated. The Farassat integral surface model which needs three-dimensional data is used, but the data are generated by coherent replication of two-dimensional data along the third dimension. To evaluate the method, a two-dimensional monopole is employed as the acoustic source and its data is replicated. It is observed that the acoustic pressure wave simulated by this method, converges to the results of two-dimensional monopole by the increase of replication length. Indeed, the pressure signal has on oscillatory behaviour by the increase of replication length while loses its amplitude during each cycle. The effects of acoustic source frequency, Mach number, location and distance of observer on the trend of convergence are investigated. Based on the results, a method to specify a suitable replication length able to simulate the pressure waves with a very good accuracy is introduced.

Keywords: Computational Aeroacoustics; Farassat method; Integral surface method; Two-dimensional integral surface.

1. Introduction

Due to the advancement of technology there has been a widespread demand to reduce the generated sound of machinery and transportation systems in a way that European governments have stated a goal for 2050 to decrease noise emission of flying aircraft by 65% [1]. To fulfill this objective, a thorough understanding of the sound generation and propagation mechanisms in the atmosphere is required. Computational aeroacoustics (CAA) is a field of study which is developed to provide this understanding. Hybrid approaches are among the most used CAA methods in industry. In these methods, computational domain is divided into two separate regions. A *near-field* region involving the distributed acoustic sources and a *far-field* region through which the acoustic waves propagate. The most challenging part in hybrid approaches is the coupling of sound propagation in these two regions. Several methods and analogies have been developed to handle this problem.

Lighthill is one of the pioneers, who introduced an analogy [2] to model sound propagation of acoustic sources. He implemented his analogy to study the generated acoustic waves emission from a free stream jet. Further analogies such as Curle [3] and Ffowcs Williams and Hawkings (FW-H) [4] have been developed to complete the Lighthill's theory and extend it to include solid body and its movement. The FW-H formulation is the most complete form of Lighthill's analogy, which consists of both surface and volume source terms. In this analogy, the computational cost is independent of the observer location. The drawback of FW-H is that it consists of volume source terms, which dramatically increases the computational cost. Therefore, aeroacoustics noise problem is expressed by scientists as a Kirchhoff problem, which its further developments lead to Kirchhoff integral surface method [5]. In this method, which is still under development [6] by defining an integral surface the quadrupole effects are taken into account without calculating any volume terms. However, the Kirchhoff method assumes that variables have a linear distribution on the integral surface. Therefore, the results of this approach are very sensitive to the selected surfaces [7]. The performed study by Singer et al. [8] reveals that the outcome of this approach may vary drastically for different integral surface locations. Another integral surface approach is Farassat method which, similar to the Kirchhoff approach, considers the quadrupole contribution on acoustic field [9]. Farassat used three-dimensional (3D) Green function to express the FW-H equation in the integral form. In this approach, Unlike the Kirchhoff method, in this approach the results are not deteriorated when nonlinearities pass through the integration surface [8]. Since the Farassat method employs 3D Green function, a 3D integral surface is needed.

In many cases, simulation of 2D acoustic field provides a reasonable estimation for the scattered acoustic waves in far-field. It is evident that the use of 2D instead of 3D simulation reduces the time and cost of computations, which makes it a suitable approach for the first design. This inspired scientists to develop two-dimensional integral form of the FW-H method, which hereafter is called two-dimensional integral surface method (TDIS) for convenience. Lockard and Guo have individually introduced two-dimensional integral form of FW-H approach, which could be coupled with 2D simulation in order to obtain an acoustic far-field solution [10,11]. They have used two-dimensional Green function to solve the FW-H equation and transformed it to frequency domain. Moreover, Bozorgi et al [12] provided an improved version by calculating the noise of a moving source in both stationary and moving media. Since, their method is developed in frequency domain, it is more cost effective than the methods developed in time domain when dealing with the narrow band noise spectrum. However, it looses its advantage when it comes to broadband noises.

Quasi-two-dimensional integral surface (QTDIS) method which is introduced by Brentner et al. [13] can simply and effectively estimate 2D acoustic signals in far-field. In this technique, the two-dimensional computational fluid dynamics (CFD) data on a curve is replicated in the third dimension in order to generate a 3D surface. Then, a 3D integral surface method is employed to estimate the radiated noise into the far-field. Brentner et al. applied this method to simulate the emission noise from a 2D circular cylinder. They used the 2D data from CFD simulation to create 3D surface data for implementing the Farassat's approach. They observed that by increasing the length of integral surface the intensity of pressure signal increases until a point, at which it starts to oscillate with decaying amplitude. Further, it is proposed that a replication length of 3 to 10 times of cylinder diameter matches the estimated sound intensity to experimental results. These researchers also concluded that the reason of having an oscillatory behaviour in sound intensity in terms of replication length is the fact that signals from each sequence of sources reach the observer point at different times [14]. Furthermore, it is proposed that the onset of this oscillation depends on the relative distance of observer and the vortex shedding frequency of the cylinder. They reported a good agreement with experiments when a replication length equals 5 times the cylinder diameter was chosen. Singer et al. utilized the QTDIS technique to analyze the acoustic field of a slat trailing-edge [8]. They replicated the 2D data along the third dimension and by implementing the Farassat method, simulated the acoustic field. They compared the quasi-two-dimensional integral surface result with

the 2D integral surface method presented by Lockard [10] and observed that the results of the QTDIS in the idealized problems converge to two-dimensional integral surface method in sufficiently long replication. Other researchers [1,16,17] reported this technique to reduce the cost of 3D simulation in the near-field. With the widespread use of this technique, based on the authors knowledge, no detailed investigation has been conducted in this regard.

From the literature, the motivations of researchers to employ QTDIS instead of TDIS method are different. Some of them used this method since it was implemented in commercial software [15,16,17]. Other tried to obtain 3D solution by adjusting the replication length [13,14]. Some knew that the two-dimensional results have greater amplitudes than those observed in the experiment but they used it as they expected to observe the same qualitative features of the acoustic waves [18]. In this research, the motivation to study QTDIS method is the fact that it provides 2D results for broadband noise more cost effective than the TDIS method, which has been developed in frequency domain.

The aim of this article is to present a methodology to specify the replication length in the quasi-two-dimensional integral surface method. For this purpose, the results of QTDIS as it is applied to a standard test case are analyzed in details and the impact of different variables on the acoustic features are investigated. A methodology based on the analyzed information from the standard test case is introduced to define the replication length value corresponding to the target convergence level. This paper is organized as follows. First, the 2D and 3D integral surface approaches which are implemented in the in-house code CAAC are described and standard benchmark tests are performed to validate the CAAC code. Next, the test cases and computational setups are presented. Then, the results are analyzed and a methodology to specify the replication length for an appropriate accuracy is introduced.

2. The 2D and 3D integral surface methods

In this investigation, the integral surface method as presented by Lockard [10] is implemented to develop the 2D part of the CAAC code. Neglecting the volumetric acoustic sources represented by the Lighthill's stress tensor, the acoustic perturbation density ρ' in the Cartesian coordinates (x_1, x_2) with orthonormal basis $\hat{e}_i$ at the observer location is given by:

$$H(f)c_0^2\rho'(\vec{x},\omega) = -\oint_{f=0} F_i(\vec{y},\omega)\frac{\partial G(\vec{x};\vec{y})}{\partial y_i}dl - \oint_{f=0} i\omega Q(\vec{y},\omega)G(\vec{x};\vec{y})dl \tag{1}$$

Which the definition of variable could be find in [10]. Fig. 1 indicates a comparison between the exact and predicted solutions for a 2D monopole at the origin of the coordinate. The comparison is conducted in two relative distances 50m and 150m between the observers and monopole. The angular frequency ω is 300rad/s, free stream Mach number equals zero, and the velocity potential amplitude A is 1m^2/s.

In the three-dimensional integral surface part of CAAC, the equations of Ghorbaniasl which are a modified version of Farassat equations are used. A suitable form of these equations and the homemade validation are presented in Ref. [19] and [20], respectively.

$$p'(\vec{x},t,\vec{M}_\infty) = p'_T(\vec{x},t,\vec{M}_\infty) + p'_L(\vec{x},t,\vec{M}_\infty) \tag{2}$$

$$4\pi p'_T(\vec{x},t,\vec{M}_\infty) = -\int_S \left[\frac{c_0 M_{\infty\tilde{R}^*}}{R^{*2}}Q\right]_e dS + \int_S \left[\frac{1}{R^*}\left(1 - M_{\infty\tilde{R}}\frac{\partial Q}{\partial t}\right)\right]_e dS \tag{3}$$

$$4\pi p'_L(\vec{x},t,\vec{M}_\infty) = \frac{1}{c_0}\int_S \left[\frac{1}{R^*}\frac{\partial L_{\tilde{R}}}{\partial t}\right]_e dS + \int_S \left[\frac{L_{\tilde{R}^*}}{R^{*2}}\right]_e dS \tag{4}$$

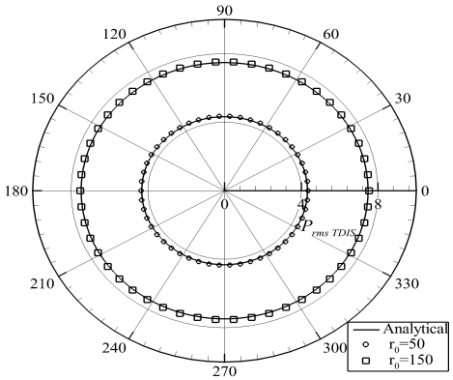

Figure 1. Comparison between the root-mean-square of the acoustic pressure P_{rms} of a 2D monopole with the the 2D part of the CAAC for two relative distances. The observers are located in the x_1x_2-plane, ω=300rad/s, and $\vec{M}_\infty = (0,0,0)$.

2.1 Computational setups and Test cases

In this study, two-dimensional monopole is employed to investigate the performance of the QTDIS approach for various replication lengths. In this method a three dimensional surface is generated with continuous replication of 2D data in the third dimension. The data on a curve is provided by the analytical solution of the 2D monopole [10] in the x_2x_3-plane. The baseline simulation has an angular frequency of 300rad/sand receiver locates at a distance of 150m and an angle of $3\pi/4$, respect to the direction of x_2-axis. A list of 26 simulations is presented in Table 1. The simulations are categorized into 6 series R, ω, Mω, MR, M_2 an Mθ. In the R-series the distance, r_o, which is defined as the distance between the centroid of the 2D surface (center of square) and receiver, varies between 100m to 250m and in the ω-series the frequency ranges from 100rad/s to 500rad/s. The MR and Mω-series are the same as the R and ω-series, respectively, except that the flow Mach number in x_2 direction is 0.5. In the M_2-series, the x_2 component of Mach number increases from 0.1 to 0.7 and in the last series Mθ, the sound pressure is estimated at different relative angle. The ambient sound velocity and density are 347.47m/s and 1.1612 kg/m^3 in all simulations, respectively.

According to the Fig. 2, the length of the surface in the x_2 and x_3 directions equals one wave length. For the 2D monopole, the flow Mach number and acoustic velocity in x_1 direction are zero. Moreover, in all simulations which are listed in Table 1, the observers are located in the x_2x_3-plane. Based on the performed mesh sensitivity analyzes, a discretization of 54 points per wave length, which provides a mesh independent solution, is used. For time discretization, the acoustic wave period is divided by 54 time intervals. The results of the simulations are presented in the following section.

3. Results and discussions

As it was mentioned in the previous section, based on the Farassat method, a three-dimensional integral surface is needed to estimate the acoustic signals in the far-field. In this section, the obtained data from the 2D monopole [10] is replicated continuously in the third dimension in order to create a 3D data surface. Consequently, the pressure signals in the far-field are estimated in terms of the replicated length. The impact of different parameters on the estimated acoustic pressure waves at various observation points are further analyzed and finally a correlation based on the replicated length to reach the required accuracy is introduced.

Table 1. List of case studies

Series	Case	ω [rad/s]	r_o [m]	M_2	θ	dx_1 [m]	dt [ms]	p_{rms} [Pa]
R	R100	300	100	0	$3\pi/4$	0.13	0.3878	5.28
	R150	"	150	"	"	"	"	4.31
	R200	"	200	"	"	"	"	3.73
	R250	"	250	"	"	"	"	3.34
ω	ω100	100	150	0	$3\pi/4$	0.40	1.1630	2.49
	ω200	200	"	"	"	0.20	0.5818	3.52
	ω300	300	"	"	"	0.13	0.3880	4.31
	ω400	400	"	"	"	0.10	0.2910	4.98
	ω500	500	"	"	"	0.08	0.2327	5.57
MR	MR100	300	100	0.5	$3\pi/4$	0.13	0.3878	10.04
	MR150	"	150	"	"	"	"	8.20
	MR200	"	200	"	"	"	"	7.10
	MR250	"	250	"	"	"	"	6.35
Mω	Mω100	100	150	0.5	$3\pi/4$	0.40	1.1600	4.73
	Mω200	200	"	"	"	0.20	0.5818	6.69
	Mω300	300	"	"	"	0.13	0.3878	8.20
	Mω400	400	"	"	"	0.10	0.2910	9.47
	Mω500	500	"	"	"	0.08	0.2327	10.58
M_2	$M_2$1	300	150	0.1	$3\pi/4$	0.13	0.3878	4.67
	$M_2$3	"	"	0.3	"	"	"	5.84
	$M_2$5	"	"	0.5	"	"	"	8.20
	$M_2$7	"	"	0.7	"	"	"	14.25
Mθ	Mθ1	300	150	0.5	$\pi/4$	0.13	0.3878	3.70
	Mθ2	"	"	"	$2\pi/4$	"	"	6.18
	Mθ3	"	"	"	$3\pi/4$	"	"	8.20
	Mθ4	"	"	"	$4\pi/4$	"	"	8.63

3.1 Oscillatory behaviour and the need for 2π replication length steps

The radiated acoustic waves from the baseline simulation, i.e. 2D monopole with the angular frequency of 300 rad/s and a distance of 150 m, are estimated. In this case, the flow Mach number is zero and the simulations are carried out for a range of replicated lengths using the 3D surface integral method of CAAC code. Figure 3 presents the root-mean-square pressure P_{rms} of acoustic waves versus the replicated length. It can be seen that P_{rms} shows an oscillatory behaviour with decaying amplitude as the replicated length increases. This oscillation in P_{rms} is observed despite of all sources along the surface integral are synchronous. The oscillatory behaviour comes from the distances between the acoustic sources and the receiver. It is obvious that the travel time of emitted signals from the sources which are located at different distances, along the x1-axis are different. The relative delay in time leads to a phase shift between the signals of each source along the replication axis, which causes a sinusoidal oscillation in P_{rms} at observer. The analytical solution of 2D monopole at receiver is also presented in Fig. 3. It is observed that the estimated P_{rms} converges to the 2D analytical solution as the surface is replicated along the third dimension. Moreover, It can be realized from this figure that for a small replication length, the estimated P_{rms} deviates significantly from analytical solution. For example, the large error zone for the current test case is the first 10m of replication where the P_{rms} is underestimated by more than 50% error. As indicated in the figure, in order to analyze and compare the convergence behaviour in different test cases, the replicated length should be selected as a length where an integer factor of 2π phase shift takes place. Here, this length is called a 2π replication length step which prevents results from oscillating. It should be pointed out that the 2π replication length step is not constant and it decreases along the replication axis. In the following, a relation to define the 2π replication length step is derived in terms of the frequency of acoustic wave and the distance between sources and observation point.

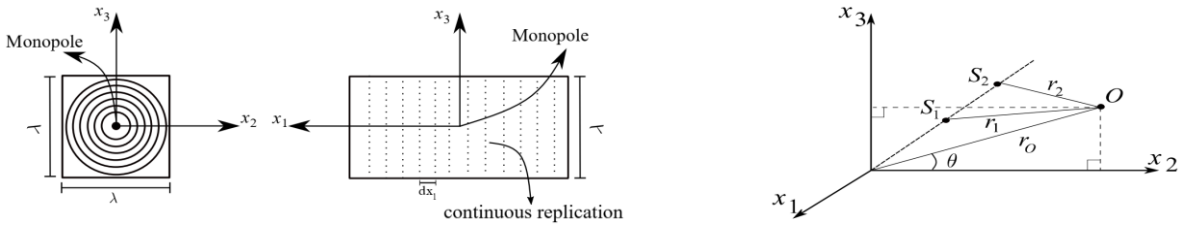

Figure 2. (a) Description of the front and right view of three-dimensional surface data used in the QTDIS method, (b) Description of relative position

Fig.2 indicates the relative position between an observer and two sources which are located in the x_1-axis. According to this figure, $\vec{r}_1$ and $\vec{r}_2$ are defined in Cartesian coordinates x_i with orthonormal basis e_i as

$$\vec{r}_1 = x_1\hat{e}_1 + r_o\cos\theta\,\hat{e}_2 + r_o\sin\theta\,\hat{e}_3 \tag{5}$$

$$\vec{r}_2 = x_1'\hat{e}_1 + r_o\cos\theta\,\hat{e}_2 + r_o\sin\theta\,\hat{e}_3 \tag{6}$$

The observer receives two sinusoidal waves emitted from the sources S_1, and S_2:

$$y_1 = \sin(\omega t), \quad t_1 \le t \le t_1 + 2\pi/\omega \tag{7}$$

$$y_2 = \sin(\omega t), \quad t_2 \le t \le t_2 + 2\pi/\omega \tag{8}$$

where t_1 and t_2 are the wave traveling time between the sources S_1 and S_2 and the receiver, respectively. The values of t_1 and t_2 are obtained from [19]. Thus, the delay time is:

$$t_2 - t_1 = \frac{\gamma^2}{c_0}\left[R_2^* - R_1^* + \vec{M}_\infty \cdot (\vec{r}_1 - \vec{r}_2)\right] \tag{9}$$

By substituting t_2 based on t_1 in (7):

$$y_1 = \sin(\omega t_1) \tag{10}$$

$$y_2 = \sin(\omega t_2) = \sin\left(\omega t_1 + \frac{\omega\gamma^2}{c_0}\left[R_2^* - R_1^* + \vec{M}_\infty \cdot (\vec{r}_1 - \vec{r}_2)\right]\right) \tag{11}$$

Thus the phase shift between the emitted waves from S_1 and S_2 is:

$$\Delta\varphi = \frac{\omega\gamma^2}{c_0}\left[R_2^* - R_1^* + \vec{M}_\infty \cdot (\vec{r}_1 - \vec{r}_2)\right] \tag{12}$$

This phase shift is due to the flow Mach number and the location of the sources. Since $\vec{M}_\infty = (0, M_2, M_3)$, the term $\vec{M}_\infty \cdot (\vec{r}_1 - \vec{r}_2)$ equals zero. Therefore,

$$R_2^* = \frac{\Delta\varphi c_0}{\omega\gamma^2} + R_1^* \tag{13}$$

By substituting R_2^* and R_1^* from Ref.[19] into (13) and rewriting the equation, the location of source S_2 with respect to S_1 on the replication axis is obtained:

$$x_1' = \left[\left(\frac{\Delta\varphi}{\omega\gamma}\right)^2 + \frac{2\Delta\varphi}{\omega\gamma}\left[(x_1^2 + r_o^2) + \gamma^2 r_o^2\left(M_2\cos\theta + M_3\sin\theta\right)^2\right]^{\frac{1}{2}} + x_1^2\right]^{\frac{1}{2}} \tag{14}$$

According to the Eq.(14) the x_1' is calculated recursively and in the first step the x_1 equals zero. Figure 3 also presents the P_{rms} versus replication length where the P_{rms} is normalized by the analyti-

cal solution. The 2π curve is the one obtained using 2π replication length step with $\Delta\varphi = 2\pi$, which converges to the analytical solution.

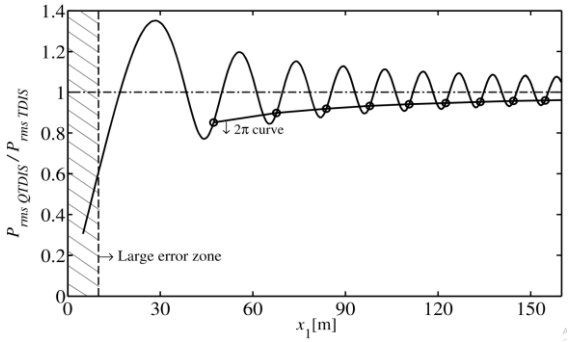

Figure 3. Oscillatory and non-oscillatory results of QTDIS with discrete error sections. $P_{rms\ TDIS}$=4.33 Pa, ω=300 rad/s and r_o = 150m

3.2 Impact of various parameters on convergence trend

In the previous section, it was shown that a surface data which is generated by the replication of a curve, can be used in the Farassat formulation to estimate the 2D acoustic emission at far-field. Based on Fig 3, the QTDIS results converge to TDIS by increase in the replication length. The convergence behaviour of this result depends on various parameters which necessitates further investigation. In this section, the impact of parameters such as frequency of acoustic wave, flow Mach number, location and distance to the observation point on the convergence behaviour are studied.

The effect of distance between the observation point and sources is investigated in Fig. 4 where the normalized P_{rms} are plotted versus the replication length. Since the result of QTDIS approach converges to TDIS solution with exponential trend, and they match at infinity; thus, the simulation are continued for an affordable length scale, means 110 times of wave length. In order to have a better comparison, P_{rms} is normalized with its maximum instead of estimated pressure of TDIS solution. The values of employed parameters in these simulations are presented in the MR-series of Table. 1 in which the distance ranges from 100 to 250 meters. It can be observed from Fig. 4 that when receiver locates near the monopole source, estimated P_{rms} by QTDIS converges faster to the analytical solution. In fact, when the observer goes further, the estimated acoustic pressure is influenced by a longer replicated surface and the contribution of the sources which locate farther from the x_2x_3-plane becomes more effective.

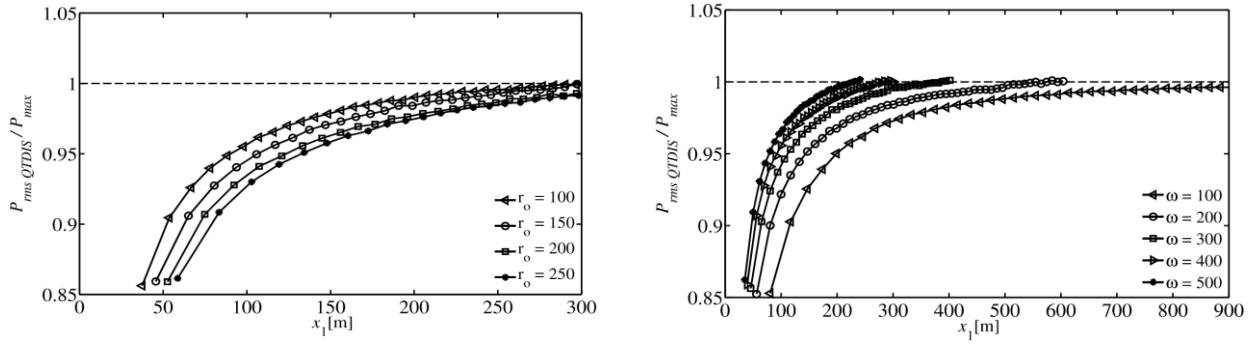

Figure 4. Comparison of convergence behaviour for ω_o =300rad/s, r_o=150m, M_2=0.5, and θ =3π/4. (a) the effects of observation distances variation , (b) the effect of source frequencies variation

Another effective parameter is frequency that its contribution to convergence behaviour is shown in Fig. 4. The presented results are corresponding to the $M\omega$-series in Table 1 in which the angular frequencies are ranging from 100rad/s to 500rad/s. It can be seen from Fig. 4 that the convergence rate increases for higher frequencies. To find the reason, the rate of decay in amplitude per cycle of oscillation is presented in Fig. 6. The vertical axis is the decay rate between two successive peaks of

oscillatory results and the horizontal axis is the number of oscillation cycle. The presented results are corresponding to the cases $M\omega 100$, $M\omega 500$, MR100, and MR250 in Table 1. It can be observed that the oscillations are exponentially attenuated and the trends are similar for all cases. Therefore, the reason of fast convergence for higher frequency signals is that the number of oscillations in terms of replication length increases.

The effect of free stream Mach number and location of observer which are corresponding to the M_2-series and $M\theta$-series are evaluated too. According to the results, the trend of convergence is not influenced by the variation of free stream Mach number and location of observer. In this section, it is shown that the replication length which is needed to reach the desired accuracy is correlated with the frequency of acoustic waves and also the distance between observation point and the source. Therefore, to specify the replication length, the frequency of waves and the distance to receiver should be taken into account.

3.3 Specifying the replication length

In order to specify the replication length, the non-dimensional parameter x^* based on the aforementioned effective parameters, i.e. frequency of waves and the distance is introduced,

$$x^* = \frac{r(x_1) - r_o}{\lambda} \tag{15}$$

where r_o is the distance between the receiver and the centroid of the 2D square in the x_2x_3-plane and the term $r(x_1) = \sqrt{x_1^2 + r_o^2}$ is the distance between the receiver and a source located at x_1 on the replicated axis. λ is the wave length, which represents the frequency effect. The results presented in Figs. 4 are replotted in Figs. 5, while the horizontal axis is scaled by x^*.

It is observed that all curves are almost coincided with each other and have the same convergence behaviour. Figure 5 shows estimated P_{rms} of all cases presented in Table 1. It can be seen; the parameter x^* is a good representative for replication length. Furthermore, the replication length corresponding to an appropriate accuracy can be extracted from this figure. Indeed, the results would be acceptably accurate if the x^* is chosen equal to 15 or more. However, the length of replication, which is calculated based on the x^*, is just an approximation of correct length. In fact, the exact length must be selected as a nearest point to the 2π replication length steps which is presented in Sec. 3.1.

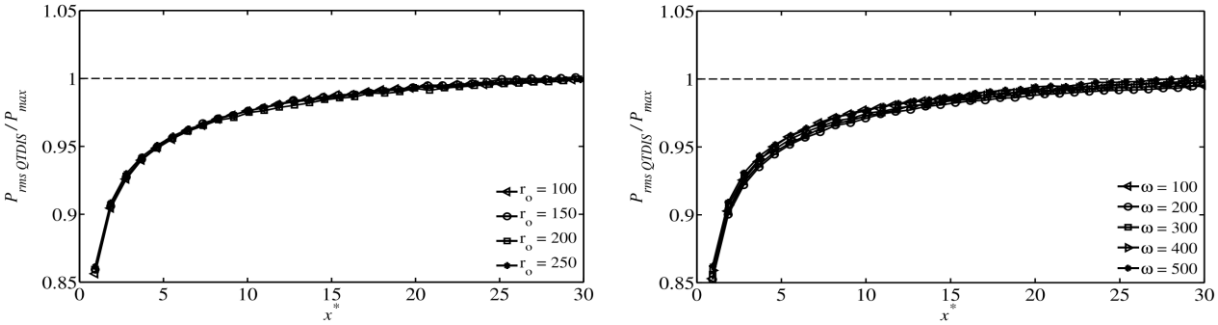

Figure 5. Comparison of convergence behaviour for ω_o =300rad/s, r_o=150m, M_2=0.5, and θ =3π/4. (a) the effects of observation distances variation , (b) the effect of source frequencies variation

4. Summary and Conclusions

In this paper, a quasi-two-dimensional integral surface method was used to simulate the radiated acoustic waves from a two dimensional monopole into the far-field. The analytical solution of a 2D monopole on a selected curve is replicated in the third dimension to generate a three-dimensional surface data. The Farassat integral surface method is then applied on the generated

surface data to estimate the acoustic pressure signal at the observation points. A detailed study was carried out to investigate the correlation between the replication length and the solutions accuracy.

The calculated sound pressure shows an oscillatory characteristic, when it is plotted versus replicated length. A primary zone along the replication axis is recognized, where a large error takes place. Also a periodic 2π phase shift is observed, when the replication length increases. This inspires to introduce a 2π replication length step, which provides a non-oscillatory curve converging to a 2D solution. The performed parametric study showed that the frequency and distance have significant contributions to the convergence behaviour of the estimated sound pressure in contrast to the observer location and the free stream Mach number. Moreover, a non-dimensional replication length in terms of frequency and relative distance was proposed, which makes an acceptable matching between the convergence trends.

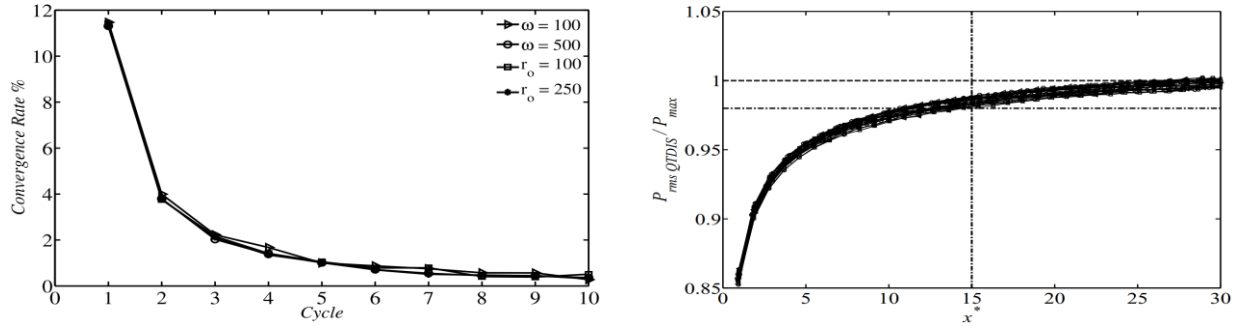

Figure 6. (a) convergence rate for cases $M\omega 100$, $M\omega 500$\$, MR100, and MR250 of Table 1. , (b) comparison of RMS of pressure which is normalized with P_{ava} versus x^*

REFERENCES

1. Flightpath, A. C. A. R. E. "2050-europe's vision for aviation." *Advisory Council for Aeronautics Research in Europe* (2011). Mallat, *A Wavelet Tour of Signal Processing*, Academic Press, New York, 1998.
2. Lighthill, Michael James. "On sound generated aerodynamically I. General theory." *Proceedings of the Royal Society of London. Series A. Mathematical and Physical Sciences* 211.1107 (1952): 564-587.
3. Curle, N. "The influence of solid boundaries upon aerodynamic sound." *Proceedings of the Royal Society of London. Series A. Mathematical and Physical Sciences* 231.1187 (1955): 505-514.
4. Ffowcs Williams, John E., and David L. Hawkings. "Sound generation by turbulence and surfaces in arbitrary motion." *Philosophical Transactions of the Royal Society of London. Series A, Mathematical and Physical Sciences* 264.1151 (1969): 321-342.
5. Farassat, F., and M. K. Myers. "Extension of Kirchhoff's formula to radiation from moving surfaces." *Journal of Sound and Vibration* 123.3 (1988): 451-460.
6. Ghorbaniasl, Ghader, Leonidas Siozos-Rousoulis, and Chris Lacor. "A time-domain Kirchhoff formula for the convective acoustic wave equation." *Proceedings of the Royal Society A: Mathematical, Physical and Engineering Sciences* 472.2187 (2016): 20150689.
7. Lyrintzis, Anastasios S. "Surface integral methods in computational aeroacoustics—From the (CFD) near-field to the (Acoustic) far-field." *International journal of aeroacoustics* 2.2 (2003): 95-128.
8. Singer, Bart, et al. "Simulation of acoustic scattering from a trailing edge." *37th Aerospace Sciences Meeting and Exhibit*. 1999.
9. Brentner, Kenneth S., and Feri Farassat. "Analytical comparison of the acoustic analogy and Kirchhoff formulation for moving surfaces." *AIAA journal* 36.8 (1998): 1379-1386.
10. Lockard, David P. "An efficient, two-dimensional implementation of the Ffowcs Williams and Hawkings equation." *Journal of Sound and Vibration* 229.4 (2000): 897-911.
11. Guo, Y. P. "Application of the Ffowcs Williams/Hawkings equation to two-dimensional problems." *Journal of Fluid Mechanics* 403 (2000): 201-221.
12. Bozorgi, Alireza, et al. "A two-dimensional solution of the FW-H equation for rectilinear motion of

sources." *Journal of Sound and Vibration* 388 (2017): 216-229.

13. Brentner, Kenneth S., et al. "Computation of sound generated by flow over a circular cylinder: an acoustic analogy approach." *NASA Conference Publication*. NASA, 1997.
14. Cox, Jared S., Kenneth S. Brentner, and Christopher L. Rumsey. "Computation of vortex shedding and radiated sound for a circular cylinder: subcritical to transcritical Reynolds numbers." *Theoretical and Computational Fluid Dynamics* 12.4 (1998): 233-253.
15. Ashcroft, G. B., K. Takeda, and Xin Zhang. "A numerical investigation of the noise radiated by a turbulent flow over a cavity." *Journal of Sound and Vibration* 265.1 (2003): 43-60.
16. Kuo, Brian C., and Nesrin Sarigul-Klijn. "Conceptual study of micro-tab device in airframe noise reduction:(I) 2D computation." *Aerospace Science and Technology* 14.5 (2010): 307-315.
17. Shao, Weidong, and Jun Li. "Analytical and numerical investigations on the aeroacoustical oscillation of flow past the cavity." *Turbo Expo: Power for Land, Sea, and Air*. Vol. 56642. American Society of Mechanical Engineers, 2015.
18. Singer, Bart A., David P. Lockard, and Kenneth S. Brentner. "Computational aeroacoustic analysis of slat trailing-edge flow." *AIAA journal* 38.9 (2000): 1558-1564.
19. Ghorbaniasl, Ghader, and Chris Lacor. "A moving medium formulation for prediction of propeller noise at incidence." *Journal of sound and vibration* 331.1 (2012): 117-137.
20. علیرضا مالکی، مجید مصباح، آرمان محسنی. "مطالعه عددی تولید و انتشار میدان صوتی حاصل از جریان حفره" هشتمین کنفرانس بین‌المللی اکوستیک و ارتعاشات، ایران، تهران، ۱۳-۱۴ آذر ۱۳۹۷.